# Dynamic Buckling Behavior for 304 Stainless Steel Columns Using Electrical LASER Alarm System

**Dr. Al-Alkawi Hussain Jasim Mohammed**
Electromechanical Engineering Department ,University of Technology/ Baghdad.
Email:Alalkawi2012@yahoo.com
**Dr. Ekbal Hussain Ali**
Email:ali_ekb@yahoo.com
Electromechanical Engineering Department ,University of Technology/ Baghdad.
**Firas Ali Jasim Al-Mahaweeli**
Iraq Telecommunication and Post Company/Baghdad.
Email:eng.firas.ali.76@gmail.com

**Received on:16/2/2015 & Accepted on:19/5/2016**

## ABSTRACT

The paper summarized some experimental main results of dynamic buckling under increasing compression load. The buckling behavior of 304 stainless steel was investigated using Euler and Johnson formulas, which is the most commonly used in industrial applications. It has been verified that metallic materials can exhibit non-linear buckling behavior with mechanical properties dependency. This behavior yield a non-linear model which based on Hong's model but using the mechanical properties with cycles to failure. It was observed that the proposed model gave safe predictions while the Hong's model yields non satisfactory predictions of critical buckling loads and also design electrical LASER alarm system to avoid the failure occurs in the specimen when access to critical buckling load.

**Keywords:** dynamic buckling, 304 stainless steel column, buckling, proposed model, LASER.

| Nomenclature | Definition | Units |
|---|---|---|
| D | Diameter of column | mm |
| ΔD | Difference in diameter | mm |
| ΔL | Difference in Gage Length | mm |
| | Yield stress | MPa |
| | Ultimate stress | MPa |
| | Initial deflection | mm |
| | Critical deflection | mm |
| E | Modulus of elasticity | GPa |
| | Effective length | mm |
| L | Actual length of column | mm |
| A | Area of cross-section | |
| S.R. | Slenderness ratio | |
| r | radius of gyration | mm |
| | No. of cycles at failure | Cycle |
| | Time of loading | Sec |
| SF | Factor of Safety | |
| | Critical buckling load | N |

## INTRODUCTION



https://doi.org/10.30684/etj.34.11A.10
2412-0758/University of Technology-Iraq, Baghdad, Iraq

Buckling analysis is an important subject for axial loaded members because the applied compressive stress at the point of failure is less than the materials ultimate compressive stress. Significant consideration must be given to the compressive load and the components geometry when designing axially compressed members in order to ensure failure will not occur for elastic instability [1].

When the column is subjected to compressive loading, the column would start at a state of balance. Critical load is the maximum compressive load that the column can take before reaching unstable equilibrium.

Any further increase in loading would result in catastrophic failure. Critical load for long and intermediate columns occurs below the elastic limits [2].

- **Avcar and address [3]** studied the elastic buckling of steel columns at different cross-sectional area, i.e. square, rectangle and circle with two different boundary conditions, i.e. fixed – free and pinned – pinned under axial compression loads. This study was carried out using finite element modeling (FEM) and numerical computations. It was found that the buckling load of pinned – pinned column is higher than fixed – pinned column. Also the buckling loads increase with the increase of the length of the column under variation of slenderness ratio for all the cross – section and boundary conditions.
- **Javidinejad and Aerospace [4]** studied the buckling behavior of an I-beam under combined axial and horizontal side loading is examined. It is shown that the actual application location of the axial loading governs the buckling behavior of the long I-beam. Theoretical formulation is developed to determine the critical buckling load for such combined loading configuration from the elastic static theory. Both, the beam deflection theoretical model and the critical load capacity are derived for this combined loading condition. The Finite Element Analysis (FEA) is utilized to apply the axial load on the beam at various configuration locations and it is shown that this application location determines the buckling behavior and the critical load of the buckling of the I-beam.
- **Alalkawi et.al. [5]** Studied the comparison of column buckling behavior between Hong model and experimental results of medium carbon steel CK35. These columns are tested under dynamic buckling with and without shot peening. The comparison Included initial imperfection, load duration and slenderness ratio of columns. The results indicated that the Hong model was capable of predict the dynamic buckling behavior of Ck35 columns.
- **Hong Hao et.al. [6]** Studied the dynamic buckling properties of imperfect columns exposure to axial intermediate velocity impact loads. The dynamic buckling equation of imperfect columns is simplified and solved. The solution of the theoretical derivative equation, according to the properties of the theoretical solution, a dynamic buckling criterion is proposed to determine the critical buckling and to estimate the dynamic buckling critical load. Hong model was examined using experimental results and it was found that good agreement is achieved with maximum percentage difference of about 5%.

This paper examined the Euler and Johnson formulas for fixed-pinned circular columns under dynamic buckling loads. The critical loads were obtained using Euler and Johnson theories for long and intermediate columns respectively. The obtained results were compared with the experimental findings and the percent errors were found for critical loads value as 5% for long and intermediate columns respectively.

## Experimental work

### Material:

The material used in the current work is 304stainless steel. This material is widely used in nuclear vessels, chemical equipment, coal hopper linings, cooking equipment, cooling coil, cryogenic vessels, dairy equipment, evaporators, flatware utensils, feed water tubing, flexible metal hose, food processing equipment, hospital surgical equipment, hypodermic needles, marine equipment and drilling operations [7].

304 stainless steel is the most widely used of all stainless steels because the chemical and mechanical properties with weld ability and corrosion/oxidation resistance provide the best all-round performance stainless steel at relatively low cost [ 8].

**Chemical composition**

Chemical analysis of the material used was done at S.C. of Geological survey and mining using X-Rays method. The results, which are compared to the American standard, are summarized in table (1).

**Table (1) chemical composition of 304 stainless steel, (wt%)**

| 304 stainless steel | *C %* Carbon | *Mn %* Manganese | *P %* Phosphorus | *S %* Sulfur | *Si %* Silicon | *Cr %* Chromium | *Ni %* Nickel | *N %* Nitrogen | *Fe* Iron |
|---|---|---|---|---|---|---|---|---|---|
| **Standard ASTM A240 [9]** | 0.08 max. | 2.00 max. | 0.045 Max. | 0.030 max. | 0.75 max. | 18.0-20.0 | 8.0-12.0 | 0.10 max. | Balance |
| **Experimental** | 0.026 | 1.72 | 0.016 | 0.021 | 0.66 | 18.9 | 9.6 | 0.07 | Balance |

**Corrosion resistance**

The metal used exhibits excellent resistance to a wide range of atmospheric, chemical, textile, petroleum and food industry exposures [9].

**Heat treatments**

Type 304 is non-hardenable by heat treatment. Annealing: Heat to 1900 - 2050°F (1038 - 1121°C), then cool rapidly. Thin strip sections may be air cooled, but heavy sections should be water quenched to minimize exposure in the carbide precipitation region. Stress Relief annealing: Cold worked parts should be stress relieved at 750°F (399°C) for 1/2 to 2 hours [9].

**Tensile properties**

The mechanical properties of (304 stainless steel) were obtained according to ASTM A370 specification. The tensile specimen can be shown in fig. (1).

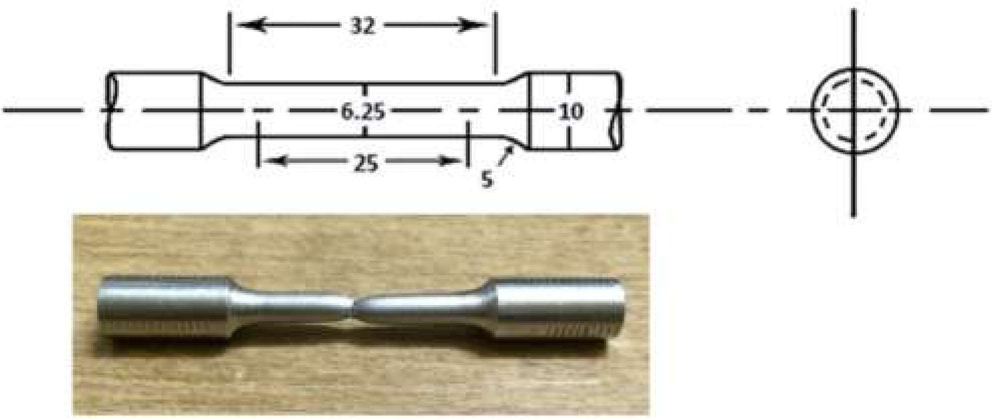


**Figure(1) Tensile test specimen (all dimensions in mm) accorded to ASTM A370 specification.**

The tensile test was conducted using the test machine WDW-200E with a capacity of 200KN shown in figure (2) in University of Technology-Material Engineering Department.


**Figure(2) Tensile test machine WDW-200E.**

The results of tensile test are shown in table (2) and figure (3).

**Table (2) gives the standard and experimantal mechanical properties.**

| 304 stainless steel | σu (Mpa) | σy (Mpa) | E (Gpa) | G (Gpa) | µ Poi.ratio | ϵ% Elongation |
|---|---|---|---|---|---|---|
| **Experimeantal** | 630 | 300 | 200 | 77 | 0.31 | 52 |
| **Standard ASTM A370 [9]** | 621 | 290 | 193-200 | 74 - 77 | 0.30 | 55 |

The above experimental results are the average of three specimens. The tensile tests are done in university of technology-material engineering department.

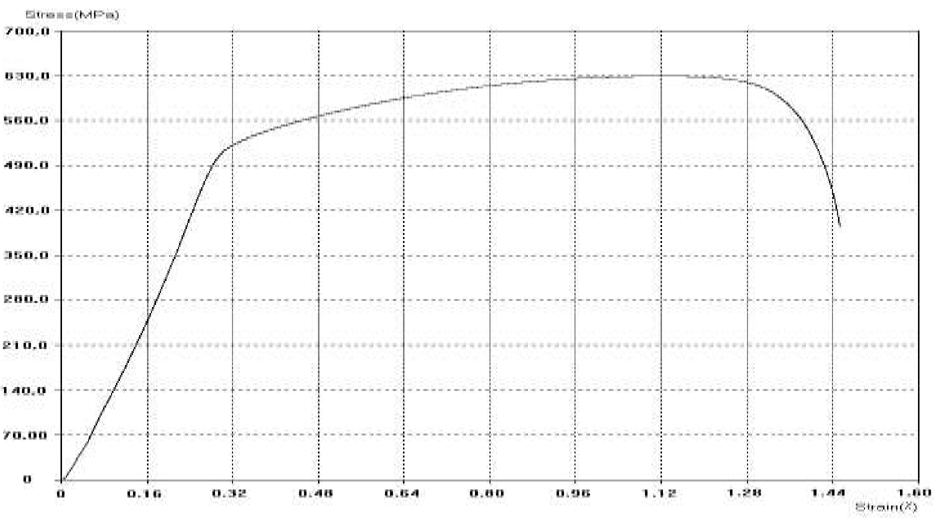


**Figure(3) tensile test results ( the above figure is the average of three specimens ).**

The poisson ratio was calculated from the equation:

$$\mu = \frac{\Delta D/D}{\Delta L/L} \qquad \text{--- --- --- (1)}$$

While the modulus of rigidity (G) was calculated by the equation:

$$G = \frac{E}{2(1+\mu)} \qquad \text{--- --- --- (2)}$$

**Buckling specimen design**

Two types of buckling specimens were prepared, long and intermediate. The dimensions of the specimens used are detailed in fig (4).

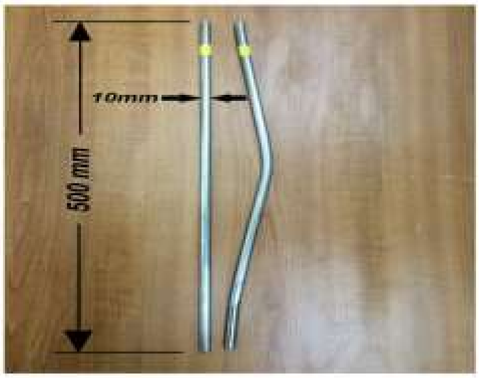


*Long column*

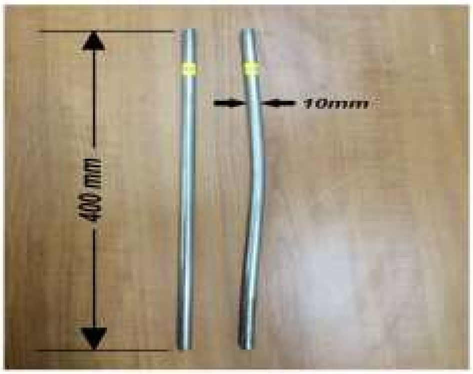


*Intermediate column*

**Figure(4) long and intermediate columns.**

The specimens were then numbered and polished. Measurement of surface roughness was carried out by means of perthometer M3A instrument. The output readings were Ra (the centre line average) and Rt (the maximum surface roughness). Table (3) gives the roughness results of three selected specimens for each type.

**Table (3) selected roughness results for buckling specimen.**

| Long specimen | | | Intermediate specimen | | |
|---|---|---|---|---|---|
| **SpecimenNo.** | **Ra (µm)** | **Rt (µm)** | **SpecimenNo.** | **Ra (µm)** | **Rt (µm)** |
| **1** | 0.28 | 1.5 | **1** | 0.45 | 2 |
| **2** | 0.44 | 1.6 | **2** | 0.26 | 1.8 |
| **3** | 0.62 | 1.9 | **3** | 0.71 | 2.2 |

Buckling analysis is normally based on the results obtained from critical load against lateral deflection curves. Thus the work is focused on the experimental work to establish this base line data from five specimens for long columns and five specimens for intermediate columns under increasing buckling compression load.

During this stage no. of cycle's data was recorded for each specimen till failure.
Failure may be defined as the instance when the specimen deformed laterally to about (1%) of the specimen length, i.e., the total laterally deflection ($\delta_{final}$=1% L). If the actual effective slenderness ratio S.R. is greater than column constant ($C_c$), then the column is long, and the Euler formula should be used to analyze the column. If the actual effective slenderness ratio S.R. is less than ($C_c$), then the column is intermediate. In these cases, Johnson formula should be used [10].

**Electrical LASER alarm system**

LASER-ray goes through long distance without scattering effect and the Ray is almost invisible. Only the radiation point and incident point is visible. So by this security project it can be make an invisible boundary of a sensitive area. There is two part of the system. One is transmitter and other is receiver.

The transmitter part is built with a LASER radiator, a pair of dry cell batteries, an on-off switch and a stand to hold on Digital Electronic Caliper. The receiver side, there is a focusing LDR (Light depending Resistor) sensor to sense the LASER continuously. The LDR sensor also holds with a stand and it connected with the main driver circuit. The circuit has two parts. One filters the signal of discontinuity ray and others is alarm circuit. When anybody crossover the invisible ray the main circuit senses the discontinuity by sensor and turn on the alarm circuit. If the alarm circuit is on it will still ringing. There are durations of ringing depends on preset timer. The system has built with low cost and high performance. The power consumption of the system is very low [11].

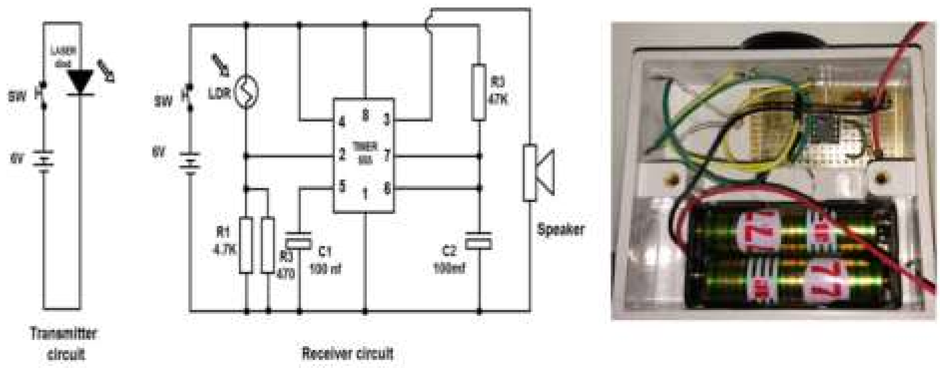


**(a) (b)**

**Figure (5) Circuit diagram of Laser security system alarm.**

When operating the LASER radiation so that the LASER beam touches the specimen, and raise the level of the LASER beam using electronic digital calipers amount of initial deflection plus 1% of the actual length of the specimen, when start test and compression is gradually applied on the specimen by a hydraulic pump of compression system, the buckling deflection will be cut off LASER beam, the alarm works (Buzzer) then the electrical motor is switched-off. The schematic diagram of electrical laser alarm system in described as in figure (5). While the actual system coupled with the buckling test rig is shown in figure (6).

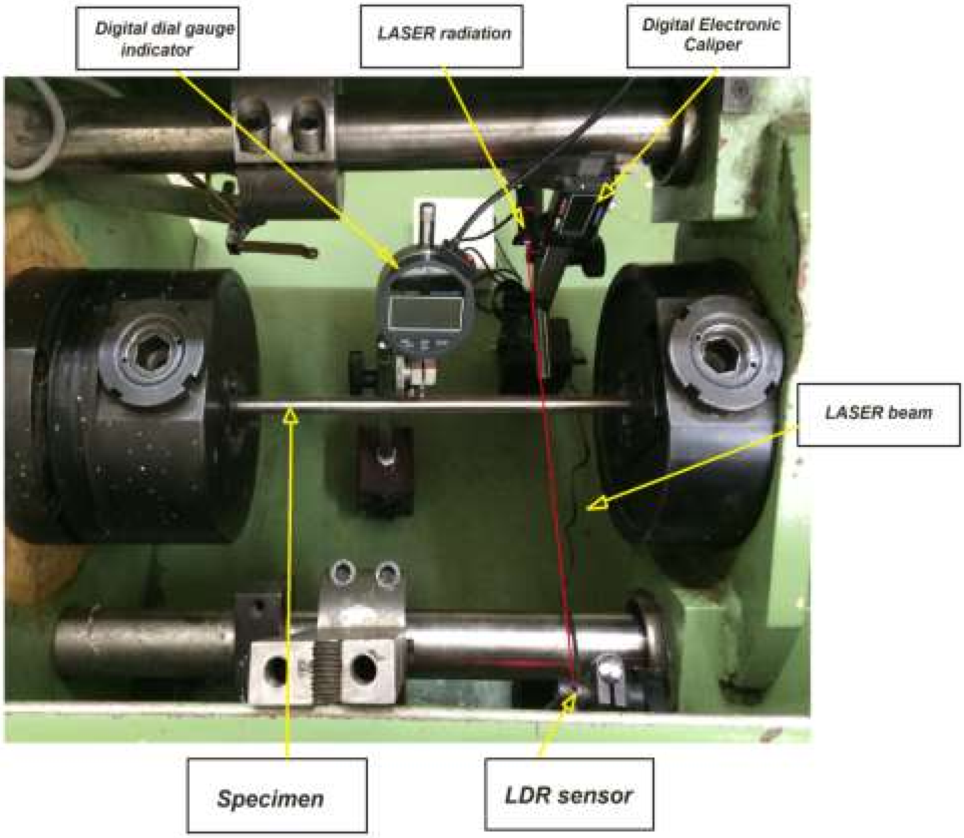


**Figure(6) Actual electrical LASER alarm system coupled with buckling test rig machine.**

Figure (7) shows the buckling test-rig machine. The rig consists of the following systems:

- Torsion system.
- Compression system.

The torsion system consists of an electrical motor of (0.5 kW), which operates with two different speeds, high speed (34 r.p.m) and low speed (17 r.p.m). When the motor starts, it gives motion in two different directions, clockwise and counterclockwise. A cycle-counter (indicating total number of cycles), is fixed on the front of the control plate. The recording digits are (99999.9) which refer to the number of cycles during test.

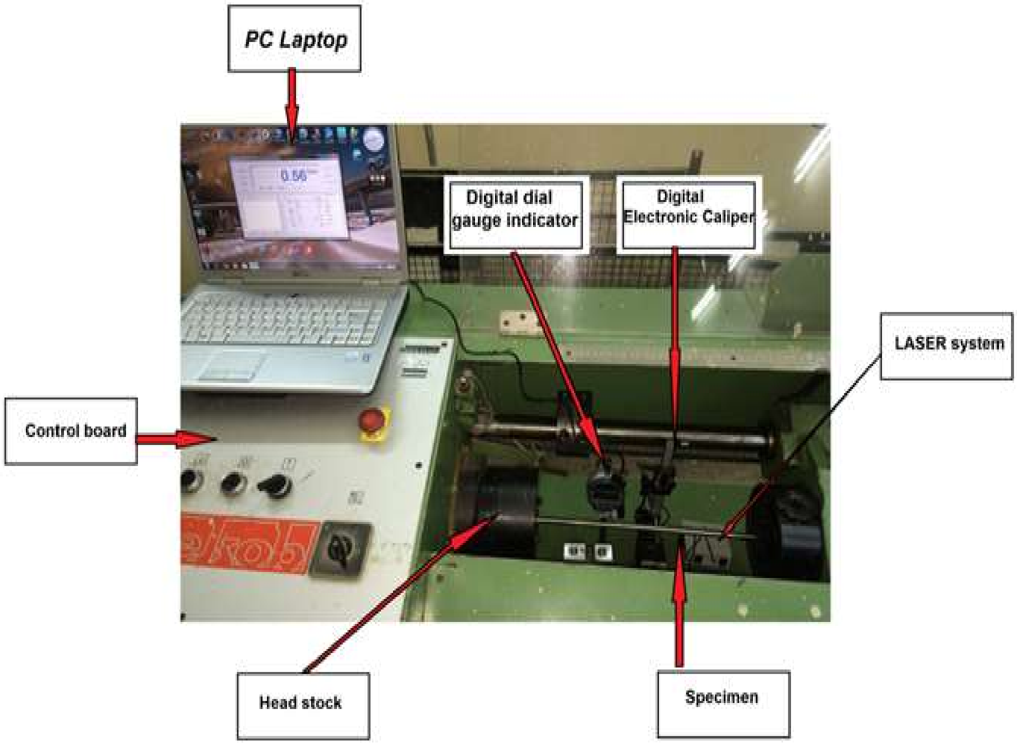


**Figure(7) the test rig for dynamic buckling rests with control panel.**

The compression system includes a manual hydraulic pump with a maximum pressure up to (315 bar). A screwed shaft is used to transfer the pressure from the hydraulic pump to the jaw which supports the specimen.
A digital dial gauge indicator is used to measure the deflection at of the specimen.

**Results and discussion**
The dynamic buckling tests were started using 20KN as a compressive load and then increased till, the critical buckling load when the alarm system start to work and then the test stop. Table (4) shows the results for five specimens tested under increasing compressive dynamic loads for long columns.

**Table (4) the columns dimensions for buckling testing.**

| No | $L_T$ mm | L mm | D mm | A mm² | I mm⁴ | R mm | S.R | Pcr N | N Cycle | δcr mm | δin mm |
|---|---|---|---|---|---|---|---|---|---|---|---|
| **1** | 500 | 420 | 10 | 78.54 | 490.9 | 5 | 117.6 | 8478 | 39.5 | 7.08 | 2.39 |
| **2** | 500 | 420 | 10 | 78.54 | 490.9 | 5 | 117.6 | 8407 | 41.9 | 6.21 | 1.99 |
| **3** | 500 | 420 | 10 | 78.54 | 490.9 | 5 | 117.6 | 8336 | 44.1 | 5.83 | 1.6 |
| **4** | 500 | 420 | 10 | 78.54 | 490.9 | 5 | 117.6 | 8393 | 42.3 | 6.21 | 1.48 |
| **5** | 500 | 420 | 10 | 78.54 | 490.9 | 5 | 117.6 | 8442 | 45.1 | 6.34 | 1.33 |

It is clear that, table (4), the critical dynamic buckling happen at the value above 8KN depend on the dimensions of columns while the No. of cycles for Pcr around 40 cycles. These findings are consistency with Ref. [10][13]. While table (5) gives the results of dynamic buckling under increasing compressive load for intermediate specimens.

**Table (5) the columns dimensions for buckling testing.**

| *No* | *$L_T$ mm* | *L mm* | *D mm* | *A $mm^2$* | *I $mm^4$* | *R mm* | *S.R* | *Pcr N* | *N Cycle* | *δcr mm* | *δin mm* |
|---|---|---|---|---|---|---|---|---|---|---|---|
| *1* | 400 | 320 | 10 | 78.54 | 490.9 | 5 | 89.6 | 11304 | 61.6 | 7.2 | 2.36 |
| *2* | 400 | 320 | 10 | 78.54 | 490.9 | 5 | 89.6 | 11162 | 61.5 | 7 | 1.68 |
| *3* | 400 | 320 | 10 | 78.54 | 490.9 | 5 | 89.6 | 11233 | 54.6 | 5.2 | 1.86 |
| *4* | 400 | 320 | 10 | 78.54 | 490.9 | 5 | 89.6 | 11198 | 59.3 | 5.33 | 2.09 |
| *5* | 400 | 320 | 10 | 78.54 | 490.9 | 5 | 89.6 | 11289 | 63.6 | 6.43 | 1.79 |

For intermediate columns, the critical dynamic buckling Pcr is observed higher than the Pcr for long columns. The intermediate columns with constant S.R. of (89.6) need more than 11KN while the long columns required slightly more than 8KN. It is obvious than the Pcr of intermediate columns larger than Pcr for long columns by about 37.5%. This conclusion agreed well with Ref. [5][12].

**Application of Hong model to the experimental present data:-**

Hong Hao et.al. [6] Proposed a dimension less theoretical model depend on several dimension less parameters which include the most dynamic buckling properties. The model may be presented in the following form:

$$\alpha_{cr} = 1 + \frac{17\pi^6 l^2 (4\sqrt{6}-\bar{\delta})}{\tau_0\, SR^2 (2\sqrt{3}+l\bar{\delta})} \quad \text{--- --- --- (3)}$$

$$\alpha_{Exp.} = \frac{P_{exp.}}{P_{cr.}} \quad \text{--- --- --- (4)}$$

$$\left\{ \begin{array}{lll} \bar{\delta} = \frac{\delta_{initial}}{r} & r^2 = \frac{I}{A} & SR = \frac{L}{r} \\ \tau_0 = \frac{t_0}{\eta} & \eta = \frac{r}{s^2 c} & c^2 = \frac{E}{\rho} \\ l = \frac{sL}{r} & s^2 = r^2 k^2 & k^2 = \frac{P_E}{EI} \end{array} \right\} \quad \text{--- --- --- (5)}$$

In which

$\alpha_{cr}$ = the dimensionless theoretical dynamic buckling critical load.

$\alpha_{Exp}$= the dimensionless experimental dynamic buckling critical load.

$P_{cr.}$: Euler critical buckling load if the column is long and Johnson Critical buckling load if the column is intermediate.

$P_{exp.}$: Experimental critical buckling load (from test rig).

$\delta_{initial}$: The maximum initial lateral deflection of column.

r: radius of gyration of column.

$t_0$: Time of loading (sec).

c: stress wave velocity of column material (m/sec).

SR: slenderness ratio of column.

$P_E$: Euler critical buckling load.

Following the above model, it can be proposed theoretical model based on the mechanical and buckling properties and initial deflection which may be written for long column in the form:

$$P_{cr} = \sigma_{cr} \,.\, A = \frac{\pi\, L_e(\delta_{in})\sigma_u * \sigma_y * (S.R)^2}{E * (N_f)^{2.5}} \quad \text{--- --- --- (6)}$$

And for intermediate column in the form:

$$P_{cr} = \sigma_{cr} \,.\, A = \frac{\pi\, L_e(\delta_{in})\sigma_u * \sigma_y * (S.R)^2}{E * (N_f)^{2}} \quad \text{--- --- --- (7)}$$

**The proposed model**

The complex nature of dynamic buckling during the service life time, decidedly to consider the entire buckling process under dynamic case as consisting of the growth of lateral deflection. This growth slow at the beginning is considered to accelerate a length of δcr . The entire cycles of reaching δcr is the number of cycles to failure. It was therefore decided to use a law of the form

$\delta = k\,(N)^{\alpha}$ --- --- --- (8)

Where δ is the lateral deflection at N cycles, k and α are constants based on experimental observations and expressed in terms of δin and δcr.

When N = 0, $\delta = \delta_{in}$ and $N = N_f$ , $\delta = \delta_{cr}$ , α was found to be approximately equal to 2.5 and 2 for long and intermediate columns respectively, and k = E in $G_{Pa}$.

The model which was proposed from data obtained by testing columns at increasing applied stress was applied to the experimental results and compared with Hong's model.

Table (6) gives the values of $P_{cr}$ and $P_{cr}$ Hong. It is observed that the $P_{cr}$ model give factor of safety for long and intermediate columns more unity up to greater than (4) in comparison with experimental results. While results obtained for Hong model shows slitily larger than the experimental, i-e the ***SF*** is so close to unity.

**Table (6) comparison of three methods experimental, Hong's model and proposed model**

| *No* | *L mm* | *$\delta in$ mm* | *$N_f$ rpm* | *$P_{cr}$ Exp. (N)* | *$P_{cr}$ Hong (N)* | *$P_{cr}$ Proposed (N)* | *SF Hong* | *SF Proposed model* | *Type Of Column* |
|---|---|---|---|---|---|---|---|---|---|
| ***1*** | 420 | 2.39 | 39.5 | 8478 | 8478.00228 | 4805 | 0.99 | 1.76 | *Long* |
| ***2*** | 420 | 1.99 | 41.9 | 8407 | 8407.40239 | 3453 | 0.99 | 2.44 | *Long* |
| ***3*** | 420 | 1.60 | 44.1 | 8337 | 8336.70255 | 2443 | 0.99 | 3.41 | *Long* |
| ***4*** | 420 | 1.48 | 46.3 | 8393 | 8393.2225 | 2001 | 0.99 | 4.19 | *Long* |
| ***5*** | 420 | 1.33 | 45.1 | 8443 | 8442.68276 | 1920 | 0.99 | 4.39 | *Long* |
| ***6*** | 320 | 2.36 | 61.6 | 11304 | 11304.00195 | 5423 | 0.99 | 2.08 | *Intermediate* |
| ***7*** | 320 | 1.68 | 61.6 | 11162 | 11162.70239 | 3873 | 0.99 | 2.88 | *Intermediate* |
| ***8*** | 320 | 1.86 | 54.6 | 11233 | 11233.35256 | 5441 | 0.99 | 2.06 | *Intermediate* |
| ***9*** | 320 | 2.09 | 59.3 | 11198 | 11198.00219 | 5183 | 0.99 | 2.16 | *Intermediate* |
| ***10*** | 320 | 1.79 | 63.6 | 11289 | 11289.87225 | 3859 | 0.99 | 2.93 | *Intermediate* |

Then the modified formulas, eq (6) and eq (7) for critical load are obtained based on Hong's model. This will produce a more accurate prediction of the buckling load. However, this may not be the most desirable design approach. In general, a design which will produce plastic deformation under the operating load is undesirable. Hence, for column which will undergo plastic deformation prior to buckling the preferred design-limiting criterion is the onset of plastic deformation, not the buckling [12].

## CONCLUSIONS

1. Hong's model gave factor of safety less than unity for all the columns tested under increasing compression load. So the above model was not satisfactory for predicate the critical buckling load.
2. The application of the present model to experimental situation has shown good agreement between prediction and experimental critical buckling loads. The proposed model gave safe prediction under all conditions of buckling tests. The actual critical load (experimental) always is being greater than the prediction by factor of safety taking values more than one to greater than four.
3. Some applications, such as airplanes, requires high factor of safety in which the present model fulfill this demand.
4. This project can be also implemented with the use of laser technology. This laser alarm is based on the interruption of Laser beam. A low cost Laser pointer is used as the source of light beam. When specimen breaks the laser path, the alarm will be generated for few seconds. Thus it is mainly used for security purposes.

## REFERENCES

[1].Anthony Beeman, 2014, “Column Buckling Analysis”, M.Sc. thesis, mechanical engineering, Rensselaer Polytechnic Institute Groton, ct.
[2].Arnold Mukuvare, 2013, “Euler Buckling”, M.Sc. Thesis, university of surrey.
[3].Mehmet Avcar, 2014, “Elastic Buckling of Steel Columns under Axial Compression”, American journal of civil engineering, vol. 2(3) p.p. 102-108.
[4].Amir Javidinejad and Zodiac Aerospace, 2012, “Buckling of Beams And Columns Under Combined Axial And Horizontal Loading With Various Axial Loading Application Location”, Journal of theoretical and applied mechanics, Sofia, vol. 42, No. 4, pp. 19–30.
[5].Al-Alkawi H. J. M., AL-Khazraji Ahmed N. and Essam Zuhier Fadhel, 2015, “Effect Of Shot Peening On Dynamic Buckling Critical Load Parameter Produced For Carbon Steel Columns”, series of engineering sciences, vol.23,No. 2,p.p. 493-500.
[6].Hong Hao, Hee Kiat Cheong and Shijie Cui, 2000, "Analysis of Imperfect Column Buckling under Intermediate Velocity Impact", international journal of solids and structures vol.37 p.p. 5297-5313.
[7].James M. Gere "Mechanics of Materials" 6th Edition, Thomson Learning, Inc. (2004).
[8].Y. Pekbey, A. Ozdamar and O. Sayman, “Buckling Optimization of Composite Columns with Variable Thickness”, Journal of Reinforced Plastics and Composites, Vol. 26, No. 13, p.p. 1337-1356, (2007).
[9]. 304 / 304L stainless steel, UNS S30400 / UNS S30403, AK Steel Corporation, 9227 center pointe drive, West Chester, OH 45069, www.aksteel.com. 2007.
[10]. K. H. AL-Jubori, 2005,” Column Lateral Buckling under Combined Dynamic Loading”, Ph.D. thesis, university of technology, technical education department.
[11].Diponkar Paul, M d. Shohel Rana and Md. Mokarram Hossain, 2012, “A Preview On Experimentation On Laser Security System”, IRACST – engineering science and technology: An international journal (ESTIJ), vol.2, No. 2,p.p. 359-366.
[12]. Joseph E. Shigley, Charles R.Mischhe, 1986,”Standard Handbook of Machine Design”, Mc Graw-hill book company.
[13].H. A. Hussein, “Buckling of Square Columns under Cycling Loads For Nitriding Steel DIN (CK45, CK67, CK101)”, Ph.D. Thesis, University of Technology, Mechanical Engineering Department, (2010).